Biochemical and Biophysical Research Communications xxx (2012) xxx–xxx

Contents lists available at SciVerse ScienceDirect

Biochemical and Biophysical Research Communications

journal homepage: www.elsevier.com/locate/ybbrc

Ahnak1 interaction is affected by phosphorylation of Ser-296 on Cavβ$_2$

Ines Pankonien [a,b], Albrecht Otto [a], Nathan Dascal [c], Ingo Morano [a,b], Hannelore Haase [a,*]

[a] Max Delbrück Center for Molecular Medicine, Department of Molecular Muscle Physiology, Robert-Rössle-Strasse 10, 13125 Berlin, Germany
[b] University Medicine Charité, Charitéplatz 1, 10117 Berlin, Germany
[c] Department of Physiology and Pharmacology, Sackler School of Medicine, Tel Aviv University, Israel Ramat Aviv, Tel Aviv 69978, Israel

ARTICLE INFO

Article history:
Received 21 March 2012
Available online xxxx

Keywords:
Ahnak
Cavβ$_2$
L-type calcium channel
PKA phosphorylation
Protein–protein interaction

ABSTRACT

Ahnak1 has been implicated in protein kinase A (PKA)-mediated control of cardiac L-type Ca^{2+} channels (Cav1.2) through its interaction with the Cavβ$_2$ regulatory channel subunit. Here we corroborate this functional linkage by immunocytochemistry on isolated cardiomyocytes showing co-localization of ahnak1 and Cavβ$_2$ in the T-tubule system. In previous studies Cavβ$_2$ attachment sites which impacted the channel's PKA regulation have been located to ahnak1's proximal C-terminus (ahnak1$^{4889–5535}$, ahnak1$^{5462–5535}$). In this study, we mapped the ahnak1-interacting regions in Cavβ$_2$ and investigated whether Cavβ$_2$ phosphorylation affects its binding behavior. *In vitro* binding assays with Cavβ$_2$ truncation mutants and ahnak1$^{4889–5535}$ revealed that the core region of Cavβ$_2$ consisting of Src-homology 3 (SH3), HOOK, and guanylate kinase (GK) domains was important for ahnak1 interaction while the C- and N-terminal regions were dispensable. Furthermore, Ser-296 in the GK domain of Cavβ$_2$ was identified as novel PKA phosphorylation site by mass spectrometry. Surface plasmon resonance (SPR) binding analysis showed that Ser-296 phosphorylation did not affect the high affinity interaction ($K_D \approx 35$ nM) between Cavβ$_2$ and the α_{1C} I–II linker, but affected ahnak1 interaction in a complex manner. SPR experiments with ahnak1$^{5462–5535}$ revealed that PKA phosphorylation of Cavβ$_2$ significantly increased the binding affinity and, in parallel, it reduced the binding capacity. Intriguingly, the phosphorylation mimic substitution Glu-296 fully reproduced both effects, increased the affinity by ≈2.4-fold and reduced the capacity by ≈60%. Our results are indicative for the release of a population of low affinity interaction sites following Cavβ$_2$ phosphorylation on Ser-296. We propose that this phosphorylation event is one mechanism underlying ahnak1's modulator function on Cav1.2 channel activity.

1. Introduction

Ca^{2+} influx through the L-type Ca^{2+} channel (Cav1.2) located in the T-tubular invaginations of the sarcolemma triggers Ca^{2+} release from the closely apposed ryanodine receptors on the sarcoplasmic reticulum leading to cardiac contraction [1]. The channel contains the pore-forming α_{1C} subunit along with accessory Cavβ$_2$ and $\alpha_2\delta$ subunits [2]. Cavβ$_2$ binds the alpha interaction domain (AID) located in the α_{1C} cytoplasmic linker connecting the first and second repeated domains (α_{1C} I–II linker). This binding is pivotal for channel trafficking to the T-tubular invaginations of the sarcolemma and for Ca^{2+} current modulation [3–5]. The increase of the Ca^{2+} current upon beta-adrenergic receptor stimulation is crucial for regulation of the heartbeat and is transmitted by protein kinase A (PKA) [6]. The causative phosphorylation sites have been recently defined to reside in the C-terminus of α_{1C} upstream of the proteolytic cleavage site [7]. Their phosphorylation is supposed to relieve the inhibitory control exerted by the proteolytically cleaved distal C-terminal fragment (CCt). Albeit the auto-inhibitory function of CCt is well documented [8,9], it is presently not clear whether CCt is steadily available for Ca^{2+} channel regulation as the CCt is reported to translocate to the nucleus serving as transcription regulator [10,11]. Thus, alternative routes of beta-adrenergic signaling may exist acting in complementary or hierarchical manner. Especially phosphorylation of Ser-478/79 on Cavβ$_2$ has been suggested to be critical for PKA-mediated upregulation of Ca^{2+} current [12,13].

Emerging evidence suggest that scaffold proteins cluster different signaling molecules leading to channel subpopulations with variable composition of modulator proteins [14]. Ahnak1 is a large membrane scaffold protein of 5890 amino acids providing docking sites for a number of proteins including cytoskeletal proteins and the Cav1 channel family [15–17]. We previously defined Cavβ$_2$ binding sites within the C-terminal ~1000 amino acids of ahnak1 [18]. Interestingly, ahnak1 peptides encompassing the Cavβ$_2$ docking sites were able to modulate Ca^{2+} channel activity [19–22]. Specifically, we found that ahnak1$^{5462–5535}$ mimicked the action of the beta-adrenergic agonist isoprenaline on Ca^{2+} current. These

* Corresponding author. Fax: +49 30 9406 2579.
E-mail addresses: i_pankonien@hotmail.com (I. Pankonien), alot@mdc-berlin.de (A. Otto), dascaln@post.tau.ac.il (N. Dascal), imorano@mdc-berlin.de (I. Morano), haase@mdc-berlin.de (H. Haase).

0006-291X/$ - see front matter © 2012 Elsevier Inc. All rights reserved.
http://dx.doi.org/10.1016/j.bbrc.2012.03.132

findings led us to suggest that the proximal C-terminus of ahnak1 acts as repressor in basal conditions by masking Cavβ_2 functionality and that this effect could be relieved by PKA phosphorylation of the interaction partners [18,20].

In the present work we focused on Cavβ_2 since recent studies revealed a more complex picture for ahnak1's implication in Ca^{2+} current regulation [21,22]. We found that ahnak1-deficient cardiomyocytes responded normally to isoprenaline excluding ahnak1 as a key regulator for beta-adrenergic increase in Ca^{2+} current [22]. But, ahnak1 emerged as additional player for Ca^{2+} channel activity regulation [21,22]. Here, we addressed the questions which Cavβ_2 regions confer binding to ahnak1's proximal C-terminus and whether it is modulated by Cavβ_2 phosphorylation. We identified Ser-296 in the GK domain of Cavβ_2 as novel PKA phosphorylation site that reduces Cavβ_2–ahnak1 interaction by eliminating and/or masking an attachment site but it does not modify the Cavβ_2–α_{1C} I–II linker interaction.

2. Materials and methods

2.1. Immunocytochemistry

Cardiomyocytes from adult mouse hearts were seeded onto laminin-coated coverslips in chamber slides (NUNC-4) and incubated for 2 h at 37 °C and 5% CO_2. Cells were washed twice with PBS, fixed for 10 min with 3.7% formaldehyde, permeabilized in PBS with 0.5% Triton X-100 for 10 min, and subsequently blocked for 30 min in PBS containing 0.2% fish skin gelatine (Sigma–Aldrich). For colocalization, the primary antibodies mouse anti-ahnak1-NT (Abnova, 5 μg/ml) and rabbit anti-Cavβ_2 (5 μg/ml) were used in combination with secondary Alexa Fluor 488-conjugated goat anti-mouse IgG (H + L, 2 μg/ml, Invitrogen) and Alexa Fluor 568-conjugated goat anti-rabbit IgG (H + L, 2 μg/ml, Invitrogen), respectively. Complete z-stacks of labeled cells were acquired using fluorescence laser scanning microscopy (LSM 510 Meta, Zeiss) and center slices were selected for display.

2.2. Recombinant proteins

Cavβ_2 constructs Cavβ_2^{1-59}, Cavβ_2^{1-228}, Cavβ_2^{1-408}, Cav$\beta_2^{195-606}$ and Cavβ_2 (GenBank ID: X64297.1, *Oryctolagus cuniculus*), Cav1.2 I–II linker and ahnak1$^{4889-5535}$ were expressed as GST fusion proteins and purified as described [15]. Ahnak1$^{5462-5535}$ was expressed as HIS fusion protein and purified using Ni–NTA Agarose (GE Healthcare, Freiburg) as described in [20]. The mutations S296A and S296E were introduced using QuickChange site-directed mutagenesis kit (Stratagene Europe, Amsterdam, The Netherlands). For binding studies between Cavβ_2 and the Cav1.2 I–II linker the GST-tag was digested from Cavβ_2 using biotinylated thrombin allowing fast and efficient removal of the protease by streptavidin-agarose (Merck, Darmstadt).

2.3. Antibodies

The antibodies against ahnak1 C-terminus, Cavβ_2-pSer-296, and Cavβ_2-pSer-478/pSer-479 were generated in rabbits and affinity-purified onto coupled ahnak1 C-terminus, the synthetic peptides SNTRS-pS-LAEVQ and QHRS-pS-pS-SAPH (Biogenes, Berlin, Germany), respectively. The ahnak1-CT antibody preparation was depleted from GST-directed antibodies.

2.4. Immunocapture assay

Wells (d = 13.2 mm) of microtiter plates (MaxiSorp, Nunc) were immobilized with 100 nM GST-tagged Cavβ_2^{1-59}, Cavβ_2^{1-228}, Cavβ_2^{1-408}, Cav$\beta_2^{195-606}$ and Cavβ_2 variants in 50 mM $NaHCO_3$ buffer, pH 9.6, for 1 h at 4 °C. The surfaces were blocked with 1 ml of blocking buffer (Candor) at 4 °C overnight followed by two washing steps with buffer A (PBS, 0.1% Tween 20). Interaction with 250 ng of recombinant ahnak1$^{4889-5535}$ was performed in buffer A containing 1% BSA and protease inhibitors (Sigma and Roche) for 3 h. After three washing steps with buffer A the proteins were harvested and run on an 8% SDS gel followed by western blot.

2.5. In vitro PKA phosphorylation

Recombinant Cavβ_2 was phosphorylated in a buffer containing 300 mM NaCl, 50 mM Na_2HPO_4 (pH 7.4), 20 mM $MgCl_2$, 0.25 mM ATP, 100 μg purified PKA catalytic subunit [15] at 30 °C for 10 min. For the control reaction $MgCl_2$ and ATP was replaced by 2 mM EDTA to inhibit phosphorylation. The reaction was stopped by exchanging to buffer A (50 mM Hepes, 150 mM NaCl, 50 mM $Na_4P_2O_7$, 25 mM NaF, 10 mM EDTA, 0.2 mM DTT, 0.05% Tween-20) using PD-10 Sephadex columns (GE Healthcare).

2.6. Identification of the phosphorylation sites by NanoLC-MS/MS

An aliquot of phosphorylated GST-tagged Cavβ_2 subunit was adjusted to pH 8.0 with 1 M Tris-buffer and digested with trypsin at 37 °C for 12 h. An UltiMate 3000 HPLC system (Dionex, Idstein, Germany) was coupled on-line to a 4000 QTRAP Mass Spectrometer (Applied Biosystems/MDS Sciex). The sample (5 μl) was loaded onto a precolumn (PepMap C18, 5 μm, 100 Å, 5 mm × 300 μm i.d., Dionex) using the autosampler of the Ultimate 3000 system. Peptides were eluted onto an analytical column (PepMap C18, 3 μm, 100 Å, 150 mm × 75 μm i.d., Dionex) and separations were performed at an eluent flow rate of 300 nL/min. Mobile phase A was 0.06% formic acid in water and B was 0.05% FA in acetonitrile–water (8:2, v/v). Runs were performed using a gradient of 1–50% B in 30 min. MS/MS analyses were conducted by using collision energy profiles chosen on the basis of the m/z value and the charge state of the parent ion. The Bioanalyst software (version 1.4.1, Applied Biosystems) was used for processing and to submit the data to the MASCOT server (version 2.1, Matrix Science Ltd., London, UK) for in-house search against the NCBInr protein database [23]. The mass tolerance of precursor ions and sequence ions was set to 0.4 Da. The searches included variable modifications of STY-phosphorylation and methionine oxidation. One missed cleavages using trypsin in a separate search cleavage without an enzyme was allowed.

2.7. Western Blot analysis

Protein samples were separated on 10% SDS polyacrylamide gels and transferred to nitrocellulose for 2 h at 300 mA. The transfers were incubated with affinity purified antibodies anti-ahnak1-CT, anti-Cavβ_2, anti-Cavβ_2-pSer-296 and anti-Cavβ_2-pSer-478/pSer-479 followed by peroxidase-coupled anti-rabbit IgG (Pierce, Rockford, IL, USA). Immunoreactive proteins were visualized by chemiluminescence (ECL) reaction (Millipore, Schwalbach).

2.8. Surface plasmon resonance (SPR) spectroscopy

SPR binding studies were performed using CM5 sensor chips in a Biacore 2000/X100 instrument (Biacore, Uppsala, Sweden) as described [22]. Ahnak1 served as ligand for the interaction with the Cavβ_2 analyte. For Cavβ_2–α_{1C} I–II linker binding anti-GST antibodies were immobilized on the chip surface to capture GST-tagged I–II linker and Cavβ_2 was applied as analyte.

Please cite this article in press as: I. Pankonien et al., Ahnak1 interaction is affected by phosphorylation of Ser-296 on Cavβ_2, Biochem. Biophys. Res. Commun. (2012), http://dx.doi.org/10.1016/j.bbrc.2012.03.132

2.9. Statistics

Statistical difference between mean values were calculated using one-way ANOVA followed by Bonferroni post hoc test and Student's *t*-test for paired values and were considered significant at *p*-values of <0.05.

3. Results and discussion

3.1. Ahnak1 and Cavβ_2 co-localize in cardiac myocyte T-tubules

We first addressed the question whether ahnak1 and Cavβ_2 co-localize in adult cardiomyocytes by immunocytochemistry. Confocal images of isolated cardiomyocytes double labeled for ahnak1 and Cavβ_2 reveal a cross-striated and punctual intracellular staining for both proteins (Fig. 1, upper panel). The merged image indicates a co-localization of ahnak1 and Cavβ_2 along T-tubular structures that is confirmed by line scan analysis (Fig. 1, lower panel). Ahnak1 localization in T-tubules appears to be specific for cardiac muscle since in skeletal muscle ahnak1 located along the peripheral sarcolemma and to costameres, but not to T-tubules [24,25]. In cardiomyocytes, we found that ahnak1 and Cavβ_2 co-localized also to perinuclear regions (Fig. 1, Merge). This is to our knowledge a novel observation offering the possibility that ahnak1 and Cavβ_2 may play a role in excitation–transcription coupling. Importantly, solely ahnak1 shows a pronounced and distinctive labeling of the peripheral sarcolemma. This localization likely reflects the role of ahnak in cytoarchitecture and in membrane resealing and repair [26–28]. Colocalization of ahnak1 and Cavβ_2 in the T-tubular invaginations of the sarcolemma provides the structural basis for ahnak1's cross-talk with the Cav1.2 channel and its role in cardiac-excitation–contraction coupling.

3.2. Mapping of ahnak1 interacting sites on Cavβ_2

We addressed the question, which sites on Cavβ_2 interact with ahnak1's proximal C-terminus (ahnak1$^{4889-5535}$) (Fig. 2C). Cavβ_2 belongs to the membrane-associated guanylate kinase (MAGUK) protein family and contains two highly conserved interacting domains, namely src-homology 3 (SH3) and guanylate kinase (GK) linked by a variable HOOK region as illustrated in Fig. 2A [4,29,30]. We created five GST-fused Cavβ_2 truncation mutants spanning the variable and conserved regions (Fig. 2B), and performed capture assays followed by Western Blot analyses using an ahnak1-directed antibody. The intensity of the ahnak1 signal captured by the full length Cavβ_2 was set to 100% and served as reference. The binding assays revealed no specific binding between the N-terminus of Cavβ_2 (Cavβ_2^{1-59}) and ahnak1$^{4889-5535}$ when compared to the negative control GST alone (Fig. 2D). The constructs Cavβ_2^{1-228} and Cavβ_2^{1-408} show interaction signals similar to the full-length Cavβ_2. Both consist of SH3 and HOOK, whereas the longer Cavβ_2^{1-408} additionally covers the GK region. While Cavβ_2^{1-228} lacking GK shows a slightly reduced binding (87%), Cavβ_2^{1-408} reaches 100% indicating that the C-terminus is dispensable for ahnak1$^{4889-5535}$ interaction. Interestingly, Cav$\beta_2^{195-606}$ that lacks SH3-HOOK and encompasses only GK and the C-terminus has a significantly reduced binding (58%). This result points to the SH3-HOOK region as playing a major role in ahnak1$^{4889-5535}$ interaction, which is supportively enhanced by the neighboring GK domain. In an additional experiment, an isolated His-tagged SH3 domain exhibited only minor binding, suggesting multivalent interactions with negative cross-talk in the SH3-HOOK-GK module to achieve the complete binding potential for ahnak1$^{4889-5535}$. It highlights the variable HOOK region that may be crucial for ahnak1 binding. Since the SH3 and GK module are highly conserved within Cavβ isoforms, they provide a basis for ahnak1 association. But, it remains to be investigated if Cavβ isoforms (e.g. Cavβ_3 and Cavβ_4) whose HOOK domain varies differ in their capability to interact with ahnak1.

3.3. Identification of Ser-296 in Cavβ_2 as novel PKA phosphorylation site

Phosphorylation of Ser-478/79 in Cavβ_2 were suggested to be critical for PKA-mediated upregulation of Ca^{2+} current in HEK cells transfected with a truncated α_{1C} and Cavβ_2 [12,13]. The mechanism was questioned by Miriyala et al. [5]. Thus, we searched for additional phosphorylation sites in Cavβ_2 and their potential impact for ahnak1 interaction. Recombinant Cavβ_2 subunit was phosphorylated by PKA and analyzed using mass spectrometry (MS). Probed on SDS–PAGE (Fig. 3A) phosphorylated Cavβ_2 revealed a migration shift of about 10 kD compared to non-phosphorylated Cavβ_2. A similar shift was observed with the truncated Cavβ_2 subunit. By MS analysis we identified the peptides ^{295}SSLAEVQSEIER^{306} and ^{478}SSSSAPHHNHR^{488} to be phosphorylated at Ser-296 and

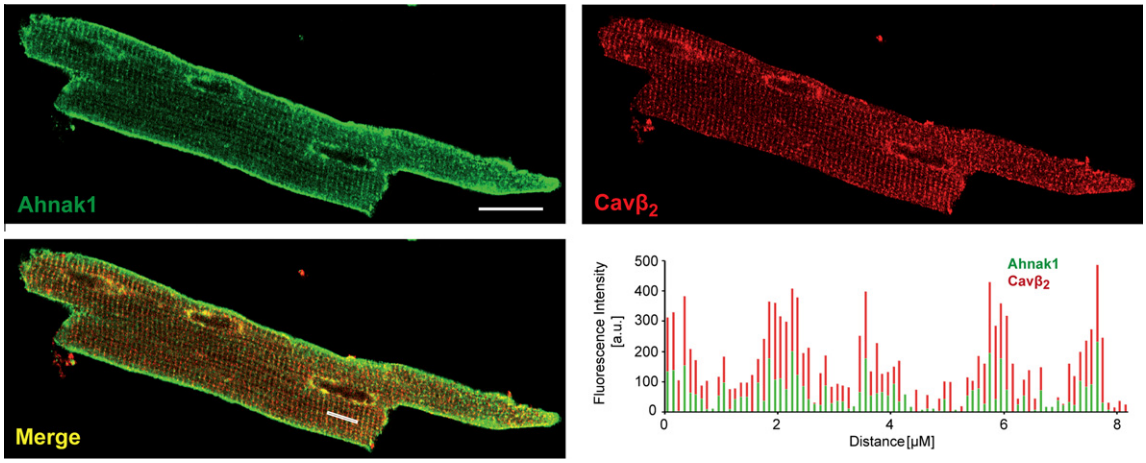

Fig. 1. Immuno-localization of ahnak1 and Cavβ_2 in mouse ventricular myocytes. Fluorescence confocal images of longitudinal sections through isolated exemplary cardiomyocytes labeled for ahnak1 (green) and Cavβ_2 (red) as indicated. The intracellular striated pattern displayed by both proteins indicates a co-localization in T-tubular structures (Merge) which is confirmed by the line scan plot demonstrating analyzed pixel intensities along the white line of the merged image. Note, a co-localization of ahnak1 and Cavβ_2 in the perinuclear compartment is observed. Ahnak1 does not co-localize with Cavβ_2 in the peripheral sarcolemma as the myocytes are outlined in green (Merge). Scale bar 30 μm.

Please cite this article in press as: I. Pankonien et al., Ahnak1 interaction is affected by phosphorylation of Ser-296 on Cavβ_2, Biochem. Biophys. Res. Commun. (2012), http://dx.doi.org/10.1016/j.bbrc.2012.03.132

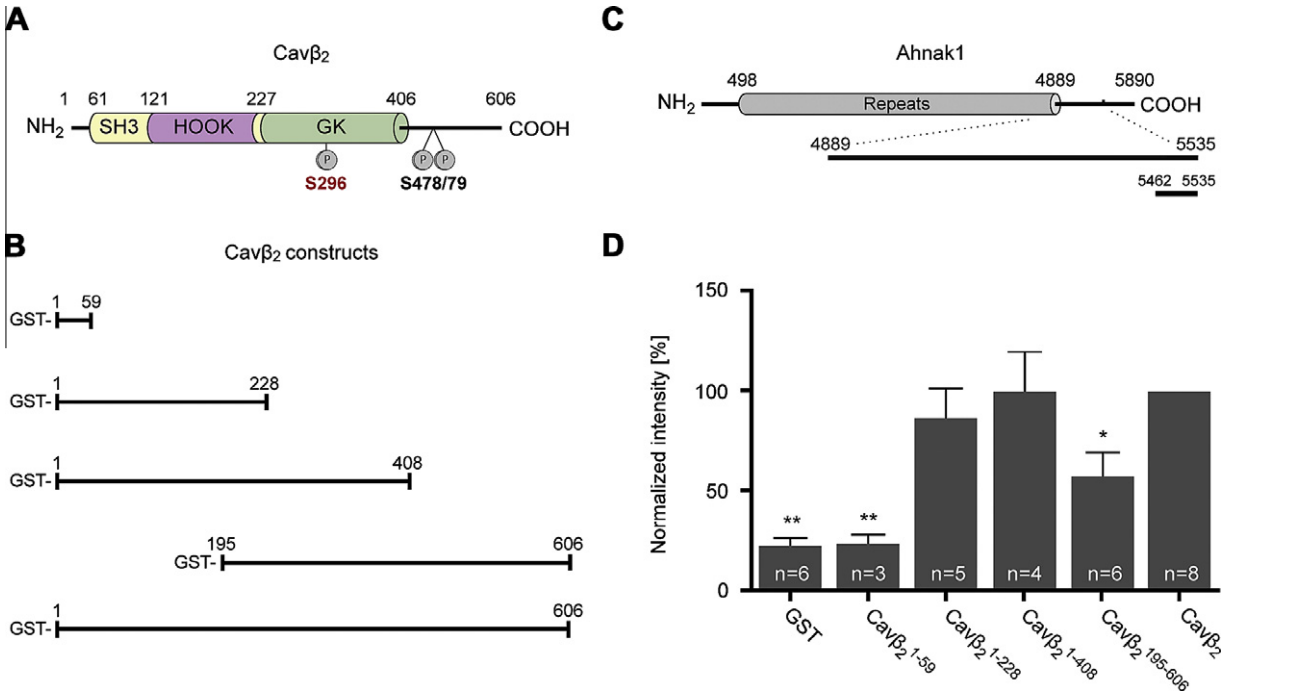

Fig. 2. (A) Molecular structure of Cavβ$_2$. (B) GST-Cavβ$_2$ constructs for ahnak1$^{4889–5535}$ interaction site mapping are shown. The Cavβ$_2^{1–59}$ construct consists of the N-terminus whereas Cavβ$_2^{1–228}$ further covers the SH3-HOOK region of Cavβ$_2$. Cavβ$_2^{1–408}$ spans the N-terminus, SH3-HOOK-GK, and lacks the C-terminus whereas Cavβ$_2^{195–606}$ encompasses only the GK domain and the C-terminus. (C) Molecular structure of ahnak1 and its proximal C-terminus applied in binding assays. (D) ELISA approach analysis of ahnak1$^{4889–5535}$ interaction with Cavβ$_2$ truncation mutants reveals significant differences, $F(5,26) = 13.13$, $p < 0.0001$; $^{**}p < 0.001$, $^{*}p < 0.05$ compared to reference Cavβ$_2$ (one-way ANOVA followed by Bonferroni post hoc test).

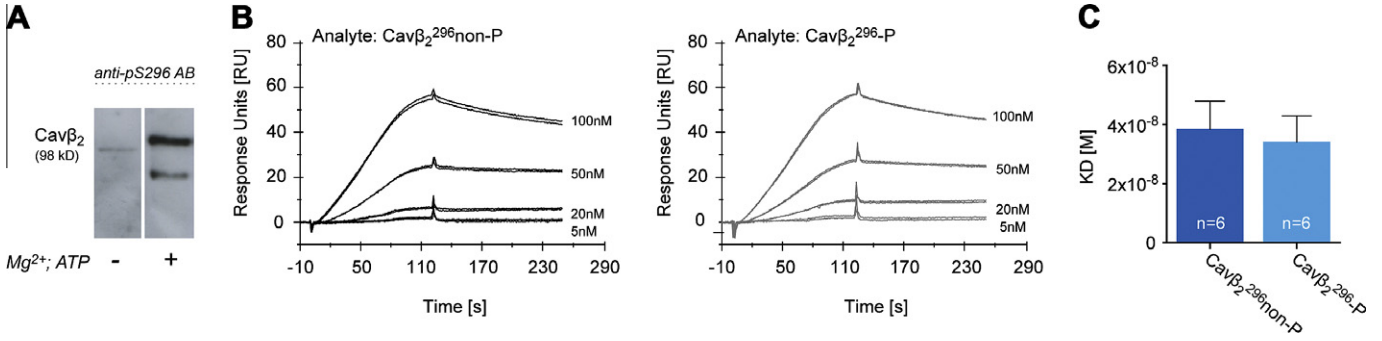

Fig. 3. (A) Western blot analysis of non-phosphorylated Cavβ$_2^{S296}$ (Cavβ$_2^{S296}$ non-P) and PKA phosphorylated Cavβ$_2^{S296}$ (Cavβ$_2^{S296}$-P) demonstrates the phosphorylation at Ser-296. (B) Representative SPR measurements between the I–II linker of Cav1.2 and Cavβ$_2^{S296}$ non-P (black curves) and Cavβ$_2^{S296}$-P (gray curves), respectively, are shown. (C) Bar graph displays K_D values of Cavβ$_2^{S296}$ non-P and Cavβ$_2^{S296}$-P indicating no significant difference.

Ser-479, respectively. We developed phospho-epitope specific antibodies directed against pSer-296 and pSer-478/pSer-479 and employed them to assess the specificity of the phosphorylation sites of Cavβ$_2$ (Fig. 3A). Importantly, Ser-296 is a novel PKA phosphorylation site within Cavβ$_2$ which, to our knowledge, is described here for the first time. Notably, the site resides within the GK domain (Fig. 2A), known to interact with the I–II linker of Cav1.2 to regulate Ca^{2+} channel activity [4,31] and ahnak1 mapped in this study.

3.4. Ser-296 phosphorylation has no effect on the interaction with the I–II linker of Cav1.2

As Ser-296 resides in the GK domain of Cavβ$_2$ (Fig. 2A) we first analyzed the potential impact of Ser-296 phosphorylation on its interaction with the I–II linker of Cav1.2. We performed real time interaction analysis by surface plasmon resonance spectroscopy (SPR). PKA was present in both cases and phosphorylation was induced by the addition of Mg and ATP. To focus only on Ser-296 we mutated Ser-479 to Ala allowing only PKA phosphorylation at Ser-296. The western blot result shows the phosphorylation of Cavβ$_2^{S296}$ (Fig. 3A). Applying SPR binding experiments non-phosphorylated and phosphorylated Cavβ$_2^{S296}$ bound the I–II linker with similar attraction (Fig. 3B, C). The high affinity values of ≈35 nM coincide well with data from previous studies [32,33] and confirm functionality of the used recombinant proteins I–II linker and Cavβ$_2$. It was reported that the high affinity interaction between both is crucial for channel trafficking; once the channel complex is incorporated into the plasma membrane, the I–II linker-Cavβ$_2$ affinity decreases [34].

3.5. Phosphorylation of Ser-296 on Cavβ$_2$ reduces its binding potential to ahnak1$^{5462–5535}$

To dissect whether phosphorylation of Ser-296 and/or Ser-479 on Cavβ$_2$ affects ahnak1$^{5462–5535}$ interaction we performed SPR binding experiments. Recombinant Cavβ$_2$ was phosphorylated by

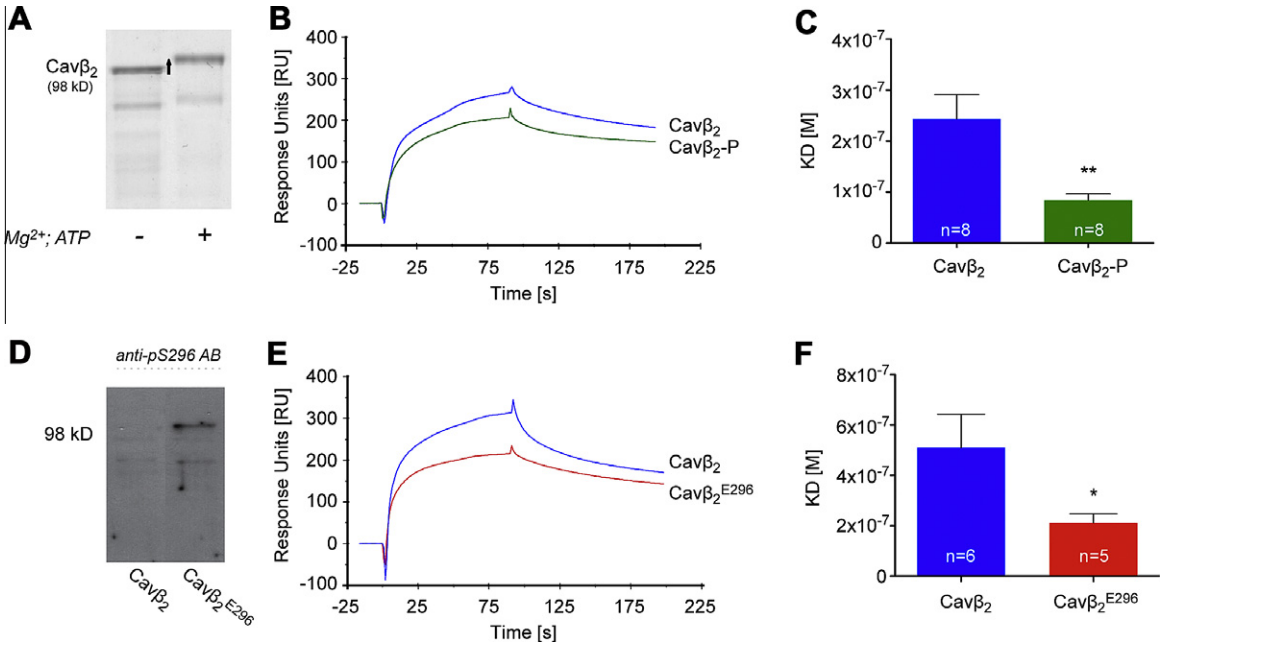

Fig. 4. (A) SDS–PAGE of Cavβ$_2$ and PKA phosphorylated Cavβ$_2$. For the phosphorylation reaction PKA in the presence or absence of Mg^{2+} and ATP, respectively, was applied. (B) Representative real-time association (0–90 s) and dissociation (90–190 s) of 4 μM of non-phosphorylated Cavβ$_2$ (Cavβ$_2$, blue) and phosphorylated Cavβ$_2$-P (Cavβ$_2$-P, green) proteins as analytes to on the sensor surface immobilized ligand ahnak1$^{5462–5535}$. (C) Bar graphs demonstrating binding affinities (K_D) of Cavβ$_2$ and Cavβ$_2$-P with ahnak1$^{5462–5535}$. (D) Western Blot analysis shows detection of Cavβ$_2^{E296}$ by a phospho-specific antibody against Ser-296. (E) Representative SPR signals demonstrating association and dissociation of Cavβ$_2$ (blue) and Cavβ$_2^{E296}$ (red) with ahnak1$^{5462–5535}$. (F) Dissociation constant (K_D) analysis for Cavβ$_2$ and Cavβ$_2^{E296}$, respectively. (For interpretation of the references to color in this figure legend, the reader is referred to the web version of this article.)

PKA representing a phosphorylation of both sites (Ser-296 and Ser-479) and subsequently passed over the ahnak1$^{5462–5535}$ protein immobilized on a biosensor chip. Real time binding revealed a significantly lower K_D value for Cavβ$_2$-P compared to non-phosphorylated Cavβ$_2$ indicating a 3-fold higher affinity between Cavβ$_2$-P and ahnak1$^{5462–5535}$ (Fig. 4B). However, the binding capacity displayed as relative binding units (RU) of ahnak1$^{5462–5535}$ and Cavβ$_2$-P is reduced by 34% compared to non-phosphorylated Cavβ (Fig. 4C). These effects provide the first evidence that Cavβ$_2$ phosphorylation by PKA modifies ahnak1$^{5462–5535}$ interaction in a complex manner. To further clarify the role of the novel identified phosphorylation site Ser-296 concerning the affected ahnak1–Cavβ$_2$ binding we substituted Ser to Ala serving as control and to Glu (Cavβ$_2^{E296}$) mimicking phosphorylation, respectively. Using the phosphospecific antibody against Ser-296 in western blot it was possible to detect the Cavβ$_2^{E296}$ variant and to discriminate it from the non-mutated Cavβ$_2$ protein (Fig. 4D). SPR binding studies gave K_D values of 510 nM and 210 nM for Cavβ$_2$ and Cavβ$_2^{E296}$, respectively, implying a 2.4-fold higher binding affinity for the Cavβ$_2^{E296}$ mutant (Fig. 4F). At the same time, ahnak1$^{5462–5535}$'s binding capacity for Cavβ$_2^{E296}$ is decreased by 60% compared to Cavβ$_2$ (Fig. 3E). Thus, phosphorylation mimic Cavβ$_2^{E296}$ reproduced the same effects of the PKA phosphorylated Cavβ$_2$ on ahnak1 interaction. Given these results we assume that Cavβ$_2$ has different populations of binding sites on ahnak1$^{5462–5535}$. PKA phosphorylation of Ser-296 may induce a conformational change to Cavβ$_2$ that eliminates or masks one set of affinity sites. It is likely that a population of lower affinity sites is lost while the high affinity site population remains. Recent studies described a phosphorylation-dependent ahnak1–Cavβ$_2$ interaction which was released after PKA phosphorylation of both binding partners accompanied with Ca^{2+} current upregulation [18,20]. We now could determine one specific phosphorylation site within Cavβ$_2$ that is responsible for a reduced binding capability to ahnak1. We suggest that phosphorylation of Ser-296 on Cavβ$_2$ may play an important role in the underlying complex mechanism of beta-adrenergic modulation by ahnak1 [22]. In summary, the phosphorylation of Ser-296 Cavβ$_2$ affects ahnak1 interaction in a complex manner and is a leading candidate for optional PKA-mediated modulation of L-type Ca^{2+} channel activity in the heart.

Acknowledgments

The study was supported by the German-Israeli Foundation for Scientific Research and Development (GIF). A special thanks goes to Dr. Patricia C. Hidalgo for providing the Cavβ$_2$-SH3 construct, Dr. Anje Sporbert (Microscopy Core Facility of the Max Delbrück Center for Molecular Medicine, Berlin) and Petra Domaing for confocal imaging. We greatly appreciate excellent technical assistance by Steffen Lutter and Karin Karczewski.

References

[1] D.M. Bers, Cardiac excitation–contraction coupling, Nature 415 (2002) 198–205.
[2] W.A. Catterall, Structure and regulation of voltage-gated Ca2+ channels, Annu. Rev. Cell Dev. Biol. 16 (2000) 521–555.
[3] Z. Buraei, J. Yang, The β subunit of voltage-gated Ca2+ channels, Physiol. Rev. 90 (2010) 1461–1506.
[4] Y.H. Chen, M.H. Li, Y. Zhang, L.L. He, Y. Yamada, A. Fitzmaurice, Y. Shen, H. Zhang, L. Tong, J. Yang, Structural basis of the alpha1-beta subunit interaction of voltage-gated Ca2+ channels, Nature 429 (2004) 675–680.
[5] J. Miriyala, T. Nguyen, D.T. Yue, H.M. Colecraft, Role of CaVbeta subunits, and lack of functional reserve, in protein kinase A modulation of cardiac CaV1.2 channels, Circ. Res. 102 (2008) e54–64.
[6] H. Reuter, A.B. Cachelin, J.E. De Peyer, S. Kokubun, Modulation of calcium channels in cultured cardiac cells by isoproterenol and 8-bromo-cAMP, Cold Spring Harb. Symp. Quant. Biol. 48 (Pt 1) (1983) 193–200.
[7] M.D. Fuller, M.A. Emrick, M. Sadilek, T. Scheuer, W.A. Catterall, Molecular mechanism of calcium channel regulation in the fight-or-flight response, Sci. Signal. 3 (2010) ra70.
[8] T. Gao, A.E. Cuadra, H. Ma, M. Bunemann, B.L. Gerhardstein, T. Cheng, R.T. Eick, M.M. Hosey, C-terminal fragments of the alpha 1C (CaV1.2) subunit associate with and regulate L-type calcium channels containing C-terminal-truncated alpha 1C subunits, J. Biol. Chem. 276 (2001) 21089–21097.
[9] A.N. Ganesan, C. Maack, D.C. Johns, A. Sidor, B. O'Rourke, Beta-adrenergic stimulation of L-type Ca2+ channels in cardiac myocytes requires the distal carboxyl terminus of alpha1C but not serine 1928, Circ. Res. 98 (2006) e11–18.

[10] N. Gomez-Ospina, F. Tsuruta, O. Barreto-Chang, L. Hu, R. Dolmetsch, The C terminus of the L-type voltage-gated calcium channel Ca(V)1.2 encodes a transcription factor, Cell 127 (2006) 591–606.
[11] E. Schroder, M. Byse, J. Satin, L-type calcium channel C terminus autoregulates transcription, Circ. Res. 104 (2009) 1373–1381.
[12] B.L. Gerhardstein, T.S. Puri, A.J. Chien, M.M. Hosey, Identification of the sites phosphorylated by cyclic AMP-dependent protein kinase on the beta 2 subunit of L-type voltage-dependent calcium channels, Biochemistry 38 (1999) 10361–10370.
[13] M. Bunemann, B.L. Gerhardstein, T. Gao, M.M. Hosey, Functional regulation of L-type calcium channels via protein kinase A-mediated phosphorylation of the beta(2) subunit, J. Biol. Chem. 274 (1999) 33851–33854.
[14] C.B. Nichols, C.F. Rossow, M.F. Navedo, R.E. Westenbroek, W.A. Catterall, L.F. Santana, G.S. McKnight, Sympathetic stimulation of adult cardiomyocytes requires association of AKAP5 with a subpopulation of L-type calcium channels, Circ. Res. 107 (2010) 747–756.
[15] A. Hohaus, V. Person, J. Behlke, J. Schaper, I. Morano, H. Haase, The carboxyl-terminal region of ahnak provides a link between cardiac L-type Ca2+ channels and the actin-based cytoskeleton, FASEB J. 16 (2002) 1205–1216.
[16] D. Matza, R.A. Flavell, Roles of Ca(v) channels and AHNAK1 in T cells: the beauty and the beast, Immunol. Rev. 231 (2009) 257–264.
[17] S.S. Carlson, G. Valdez, J.R. Sanes, Presynaptic calcium channels and alpha3-integrins are complexed with synaptic cleft laminins, cytoskeletal elements and active zone components, J. Neurochem. 115 (2010) 654–666.
[18] H. Haase, Ahnak, a new player in beta-adrenergic regulation of the cardiac L-type Ca2+ channel, Cardiovasc. Res. 73 (2007) 19–25.
[19] J. Alvarez, J. Hamplova, A. Hohaus, I. Morano, H. Haase, G. Vassort, Calcium current in rat cardiomyocytes is modulated by the carboxyl-terminal ahnak domain, J. Biol. Chem. 279 (2004) 12456–12461.
[20] H. Haase, J. Alvarez, D. Petzhold, A. Doller, J. Behlke, J. Erdmann, R. Hetzer, V. Regitz-Zagrosek, G. Vassort, I. Morano, Ahnak is critical for cardiac Ca(V)1.2 calcium channel function and its beta-adrenergic regulation, FASEB J. 19 (2005) 1969–1977.
[21] J.L. Alvarez, D. Petzhold, I. Pankonien, J. Behlke, M. Kouno, G. Vassort, I. Morano, H. Haase, Ahnak1 modulates L-type Ca(2+) channel inactivation of rodent cardiomyocytes, Pflugers Arch. 460 (2010) 719–730.
[22] I. Pankonien, J.L. Alvarez, A. Doller, C. Kohncke, D. Rotte, V. Regitz-Zagrosek, I. Morano, H. Haase, Ahnak1 is a tuneable modulator of cardiac Ca(v)1.2 calcium channel activity, J. Muscle Res. Cell Motil. (2011).
[23] D.N. Perkins, D.J. Pappin, D.M. Creasy, J.S. Cottrell, Probability-based protein identification by searching sequence databases using mass spectrometry data, Electrophoresis 20 (1999) 3551–3567.
[24] U. Zacharias, B. Purfurst, V. Schowel, I. Morano, S. Spuler, H. Haase, Ahnak1 abnormally localizes in muscular dystrophies and contributes to muscle vesicle release, J. Muscle Res. Cell Motil. 32 (2011) 271–280.
[25] A. Marg, H. Haase, T. Neumann, M. Kouno, I. Morano, AHNAK1 and AHNAK2 are costameric proteins: AHNAK1 affects transverse skeletal muscle fiber stiffness, Biochem. Biophys. Res. Commun. 401 (2010) 143–148.
[26] Y. Huang, S.H. Laval, A. van Remoortere, J. Baudier, C. Benaud, L.V. Anderson, V. Straub, A. Deelder, R.R. Frants, J.T. den Dunnen, K. Bushby, S.M. van der Maarel, AHNAK, a novel component of the dysferlin protein complex, redistributes to the cytoplasm with dysferlin during skeletal muscle regeneration, FASEB J. 21 (2007) 732–742.
[27] A. Rezvanpour, L. Santamaria-Kisiel, G.S. Shaw, The S100A10-annexin A2 complex provides a novel asymmetric platform for membrane repair, J. Biol. Chem. (2011).
[28] C. Benaud, B.J. Gentil, N. Assard, M. Court, J. Garin, C. Delphin, J. Baudier, AHNAK interaction with the annexin 2/S100A10 complex regulates cell membrane cytoarchitecture, J. Cell Biol. 164 (2004) 133–144.
[29] F. Van Petegem, K.A. Clark, F.C. Chatelain, D.L. Minor Jr., Structure of a complex between a voltage-gated calcium channel beta-subunit and an alpha-subunit domain, Nature 429 (2004) 671–675.
[30] M. De Waard, M. Pragnell, K.P. Campbell, Ca2+ channel regulation by a conserved beta subunit domain, Neuron 13 (1994) 495–503.
[31] H.M. Colecraft, B. Alseikhan, S.X. Takahashi, D. Chaudhuri, S. Mittman, V. Yegnasubramanian, R.S. Alvania, D.C. Johns, E. Marban, D.T. Yue, Novel functional properties of Ca(2+) channel beta subunits revealed by their expression in adult rat heart cells, J. Physiol. 541 (2002) 435–452.
[32] A.C. Dolphin, Beta subunits of voltage-gated calcium channels, J. Bioenerg. Biomembr. 35 (2003) 599–620.
[33] S. Geib, G. Sandoz, K. Mabrouk, A. Matavel, P. Marchot, T. Hoshi, M. Villaz, M. Ronjat, R. Miquelis, C. Leveque, M. de Waard, Use of a purified and functional recombinant calcium-channel beta4 subunit in surface-plasmon resonance studies, Biochem. J. 364 (2002) 285–292.
[34] C. Canti, A. Davies, N.S. Berrow, A.J. Butcher, K.M. Page, A.C. Dolphin, Evidence for two concentration-dependent processes for beta-subunit effects on alpha1B calcium channels, Biophys. J. 81 (2001) 1439–1451.

Please cite this article in press as: I. Pankonien et al., Ahnak1 interaction is affected by phosphorylation of Ser-296 on Cavβ_2, Biochem. Biophys. Res. Commun. (2012), http://dx.doi.org/10.1016/j.bbrc.2012.03.132